DESIGN AND CHARACTERIZATION OF THE POWER COUPLER LINE FOR HIE-ISOLDE HIGH BETA CAVITY

A. D'Elia*, Cockroft Institute, UK and University of Manchester, Manchester, UK
M. Pasini, CERN, Geneva, Switzerland
and Instituut voor Kernen Stralingsfysica, K. U. Leuven, Leuven, Belgium

Abstract

The first stage of the planned upgrade of the ISOLDE facility at CERN will provide a boost in beam energy from 3MeV/u up to 5.5MeV/u [1]. In order to reach this goal, it is planned to install downstream the present structure a superconducting linac based on two gap independently phased Nb sputtered Quarter Wave Resonators (QWRs) working at 101.28MHz. The design parameters foresee to have a power dissipated on the cavity wall of 7W with a Q_0=6.6·10^8 for an accelerating field of 6MV/m. The cavity will be fed via a moveable antenna that, in operating condition, is designed to reach a maximum overcoupled condition of a factor 130 (rms power flowing in the coupler line of 230W) in order to get a bandwidth at the resonant frequency of ≈20Hz. A wide dynamic range (Q_{ext} ranging from 10^4 to 10^9) is requested in order to allow tests and conditioning both at room temperature and in superconducting operating mode. A "dust free" sliding mechanism has been integrated in the mechanical concept which will be presented below together the full e-m analysis of the coupler line.

INTRODUCTION

The HIE-ISOLDE cavities will be constructed by making use of the Nb/Cu sputtering technology [2]. The use of copper permits to have massive and stiffer cavities which reduces microphonics effects, and prevents the deformations due to the mechanical actions of the tuning system, at a fraction of the cost, compared to bulk niobium technology. The main parameters of HIE-ISOLDE cavity are shown in Table 1 [3].

As mentioned in [4], a common practice for choosing the loaded bandwidth is to consider six times the rms microphonic noise plus twice the resolution of the mechanical tuner. The microphonic noise is estimated to be less then 1.5Hz, based on Legnaro experience [5], and we foresee a tuner sensitivity of ≈1.25Hz. Then, the expected loaded bandwidth should be of ≈11.5Hz. We have chosen a coupling coefficient β=130, giving a bandwidth of Δ_f ≈20Hz, to stay in a safer margin. The forward power will be of P_f ≈230W rms.

However a sliding mechanism has also to be foreseen both in order to perform tests and conditioning at different temperatures and in case of slight changes in the cavity measured parameters.

* Alessandro.Delia@cern.ch

Table 1: Cavity parameters.

Frequency (MHz)	101.28
β (%)	11.4
U	7.4J
E_{acc} (MV/m)	6
L_{norm} (mm)	300
E_{peak}/E_{acc}	5.4
B_{peak}/E_{acc} [G/(MV/m)]	96
R_{sh}/Q_0 (Ω)	554
g=$R_s \cdot Q_0$ (Ω)	30.34
P_{cav} (W)	7
R_s (nΩ)	46

A capacitive coupler has been chosen to couple the electromagnetic power to the cavity. Its position is shown in Fig. 1 where also the layout of the whole line is presented.

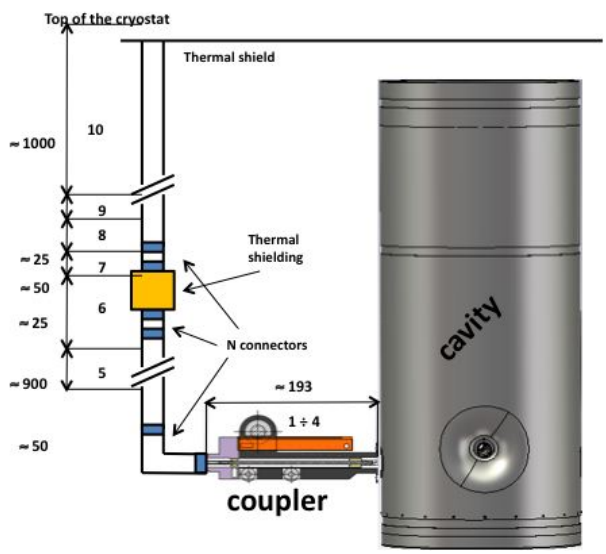

Figure 1: Coupler line layout: the full line has been divided in 10 parts, dimensions are in mm.

In the following the mechanical design of the coupler will be described. The analysis of the RF line with the power dissipated distribution will be fully reported. Finally we will describe the method we use to measure the external Q of the coupler and pick-up.

COUPLER MECHANICAL DESIGN

The cleanliness of the cavity environment is fundamental to reach the optimum performances. Therefore it is very important to provide for a "dust free" sliding mechanism.

Figure 2 shows a 3D view of the coupler when fully inserted (Fig. 2 a)) or fully extracted (Fig. 2 b)). Figure 3 shows a cut view of the coupler along the axis in which the wheels providing for the sliding motion are visible. This solution minimizes the powder production because of the wheel mechanism. Furthermore, as the motion happens on the external part of the outer conductor, if some dust is produced, it has no possibilities of falling down on the inner part and then to soil the cavity. The internal antenna is made in copper while the rest of the body is in stainless steel. Two pieces of MACOR are used for mechanical stability and alignment.

The total stroke is of 70mm, giving an insertion length of $-10\text{mm} \leq L_{in} \leq 60\text{mm}$, for a quite large dynamic range of $7 \cdot 10^3 \leq Q_{ext} \leq 5 \cdot 10^9$.

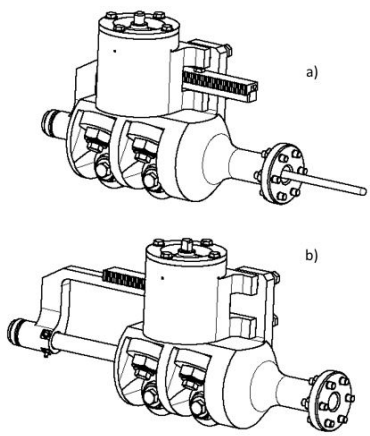

Figure 2: 3D view of the coupler when fully inserted, a), or fully extracted, b).

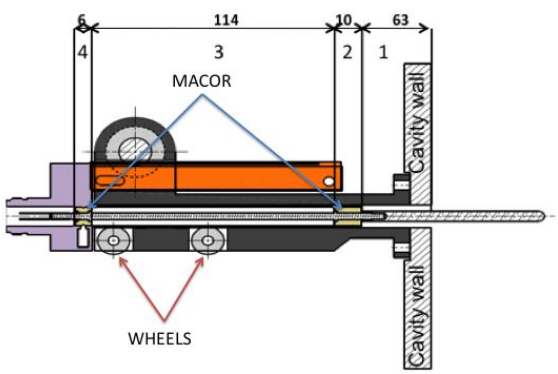

Figure 3: Mechanical layout of the coupler. The coupler line has been divided in 4 pieces: pieces 2 and 4 are filled with MACOR, the dimensions are relative for β=130 and are in mm.

ELECTROMAGNETIC SIMULATIONS

The coupler has been simulated by using MWS [6].

The result curve is shown in Fig. 4: a coupling of β=130 should be reached for an insertion length of ≈10mm while the critical coupling at room temperature for a length of ≈50mm. The design foresees also to reach the critical coupling when the cavity is superconducting.

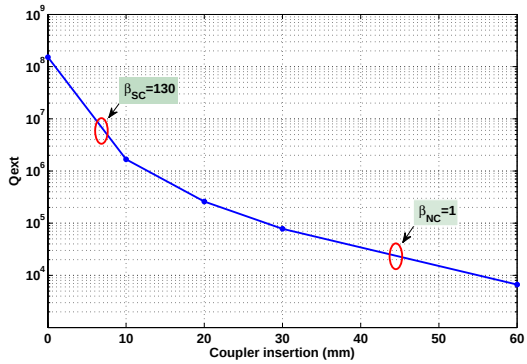

Figure 4: Result of a parametric simulation by MWS showing the behavior of Q_{ext} for different penetration of the antenna; the critical coupling at room temperature should happen around 45mm while the desired condition of β=130 should be reached for a penetration length of about 10mm.

The penetration of the coupler inside the cavity will change also the resonant frequency. In Fig. 5 the behavior of this change coming from a set of measurements is shown. It has to be noticed that for penetration length less than 22mm the change in frequency starts to be negligible.

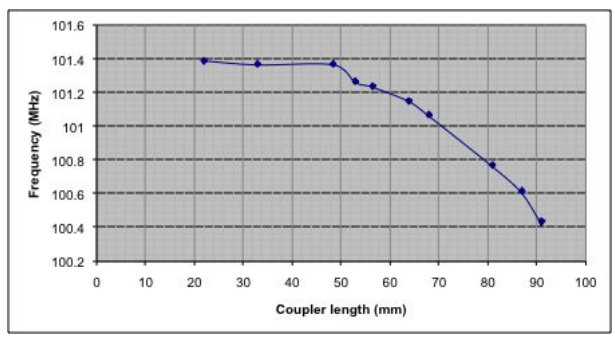

Figure 5: Resonant frequency as a function of the coupler penetration length.

LINE ANALYSIS

As written above, the line has been divided in 10 parts dependently on the different geometrical and electromagnetic behaviors. The line has been treated as described in [7] and [8]. We assume a TEM mode propagating along the line and we assume also that the line is loaded by the antenna, as shown in Fig. 6. We will express this load in terms of reflection coefficient $\Gamma_L = \frac{1-\beta}{1+\beta}$ and then we will

propagate this load along the line in order to get the full voltage and current profiles.

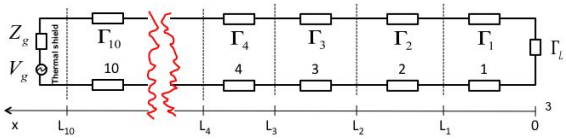

Figure 6: Model of the coupler line used for the calculation: the line has been divided in 10 parts and we move back from the load characterized by its reflection coefficient Γ_L, towards the generator.

The reflection coefficient will propagate in each piece of the line as $\propto e^{-2\gamma_i x}$ and it has also to be provided for its continuity on the interfaces between two different pieces of line. Therefore we get

$$\Gamma_i(x) = A_i e^{-2\gamma_i x} \tag{1}$$

where the coefficient A_i takes into account the continuity of Γ along the line and it can be expressed as

$$\begin{cases} A_1 = \Gamma_L \\ A_i = \Gamma_{i-1}(L_{i-1}) e^{\gamma_i L_{i-1}} \quad \text{for } i = 2, \ldots, N \end{cases} \tag{2}$$

In the above equations, γ_i is the propagation coefficient equal to

$$\gamma_i = \alpha_i + j\beta_i \quad \text{with} \begin{cases} \alpha_i = \alpha_{ic} + \alpha_{id} \\ \beta_i = \frac{2\pi}{\lambda_0}\sqrt{\epsilon_{ir}} \end{cases}, \tag{3}$$

where α_i is the attenuation constant due to the losses into conductors (α_{ic}) and into dielectrics (α_{id}); β_i is the propagation constant which depends on the wavelength λ_0 and on the dielectric permittivity, ϵ_{ir}, of the medium. More in details, the expression of the attenuation constants is the following

$$\begin{cases} \alpha_{ic} = \dfrac{1}{4\pi Z_{ic}} \left[\dfrac{R_{si_i}}{a} + \dfrac{R_{so_i}}{b} \right] \\ \alpha_{id} = \dfrac{\pi f}{c} \tan\delta_i \end{cases} \tag{4}$$

where Z_{ic} is the line impedance, R_{si_i,so_i} is the surface resistance of the inner or outer conductor, respectively, a and b are the radii of the inner and outer conductor, respectively, and $\tan\delta_i$ is the loss tangent of the dielectric. As $\alpha_{ic} \propto \sqrt{f}$ while $\alpha_{id} \propto f$, at low frequencies the contribution of the losses in the dielectrics is negligible.

Finally, rewriting the solution of the *telegraph's equations* in terms of the reflection coefficient we can get the profile of the voltage and current for each piece of the line as

$$\begin{cases} V_i(x) = V_i^+ \cdot e^{\gamma_i x} \left[1 + \Gamma_i(x)\right] \\ I_i(x) = I_i^+ \cdot e^{\gamma_i x} \left[1 - \Gamma_i(x)\right] \end{cases} \tag{5}$$

The terms V_i^+ / I_i^+ can be found by imposing the continuity on the interfaces which gives

$$\begin{cases} V_1^+ = \sqrt{2 Z_{c1} P_f} \\ I_1^+ = \sqrt{2\frac{P_f}{Z_{c1}}} \end{cases} \text{and} \begin{cases} V_i^+ = V_{i-1}^+ e^{L_{i-1}(\gamma_{i-1} - \gamma i)} \\ I_i^+ = I_{i-1}^+ e^{L_{i-1}(\gamma_{i-1} - \gamma i)} \end{cases} \tag{6}$$

with $i = 2, \ldots, N$; P_f in our case is equal to ≈230W and $Z_{c1} \approx 50\Omega$.

Voltage, current and Γ profile along the line is shown in Fig. 7

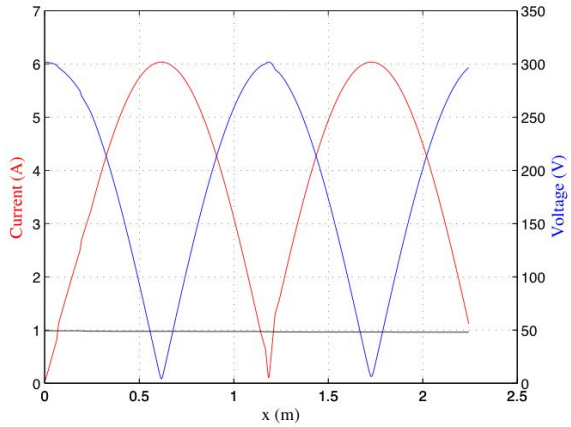

Figure 7: Behavior of the voltage (blue), current (red) and reflection coefficient Γ (black) along the line.

The active power dissipated in the line will be derived from the profile of the voltage and current as

$$P_d(x) = \frac{1}{2} \Re \left\{ V(x) \overline{I}(x) \right\}. \tag{7}$$

This represents the total power dissipated in the line, by subtracting the 7W absorbed by the load, we have the ohmic power dissipated only in the transmission line. The results are shown in Fig. 8.

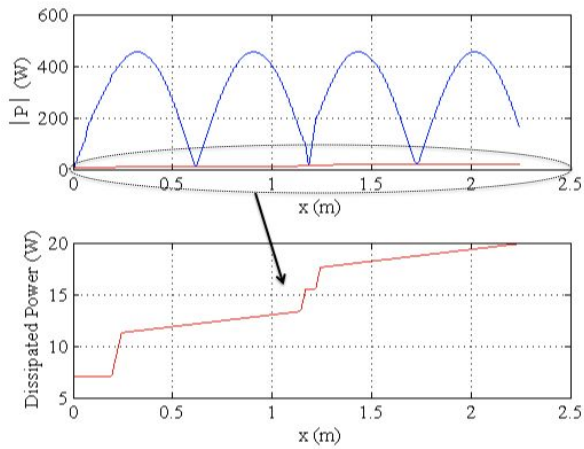

Figure 8: Behavior of the absolute value of the power flowing along the line (top plot); behavior of the dissipated power along the line (bottom plot).

Table 2: Dissipated power in the coupler line.

Piece	P_{out} (W)	P_{in} (W)	P_{tot} (W)
1	0.0195	0.045	0.0645
2	0.0105	0.029	0.0395
3	0.035	0.096	0.131
4	0.006	0.0175	0.0235
5	1.269	2.922	4.191
6	0.533	1.5325	2.065
7	0.635	1.4615	2.097
8	0.0055	0.067	0.0725
9	0.635	1.462	2.097
10	0.593	1.704	2.297
Total	**3.742**	**9.337**	**13.079**

In Table 2 the numerical values of the power dissipation on the different pieces of the line are shown. The values for inner and outer conductor dissipations are derived by considering that the total power dissipated on the conductors is the sum of inner and outer dissipated power and that the power dissipated on each conductor is inversely proportional to its radius and to the square root of its conductivity.

As final remark, the N connectors have to be inserted in the current node positions, when possible, in order to minimize the losses coming from bad contacts.

Q_{EXT} MEASUREMENTS

Measurements at room temperature are important to test and calibrate the coupler and pick-up. Usually, around critical coupling with β=1, it is possible to obtain the value by a measurement of S11. When the system becomes highly undercoupled, due to the very high Q_{ext}, to get reliable results by a S11 measurement becomes difficult. A possible method to ride out the *impasse* is presented in the following. This method has been developed to measure the Q_{ext} of the pick-up by measuring S21 by feeding by the coupler, but, due to the symmetry of the system it is obviously possible to feed by the pick-up and measuring the coupler.

From the power balance Pin=Pf-Pr=Pc+Pe (see Fig. 9) and considering that Pr=$\left[1-\left(\frac{\beta_c-1}{\beta_c+1}\right)^2\right]$, we can write the relation

$$\beta_{pu}=\frac{|S21|^2}{\frac{4\beta_c}{(\beta_c+1)^2}+|S21|^2}. \quad (8)$$

where, β_{pu}, is the coupling coefficient of the pick-up and β_c, is the coupling coefficient of the coupler.

Therefore, $Q_{ext_{pu}}$ can be measured in four simple steps:

1. Measuring β_c by S11:

$$\beta_c=\begin{cases}\text{SWR if } \beta_c\geq 1\\ 1/\text{SWR if } \beta_c<1;\end{cases}$$

2. Measuring S21, from which, one gets β_{pu} from eq. 8;
3. Getting Q_0 from the relation $Q_0=Q_{load}(1+\beta_c+\beta_{pu})$;
4. Getting $Q_{ext_{pu}}$ from the relation $\beta_{pu}=Q_0/Q_{ext_{pu}}$.

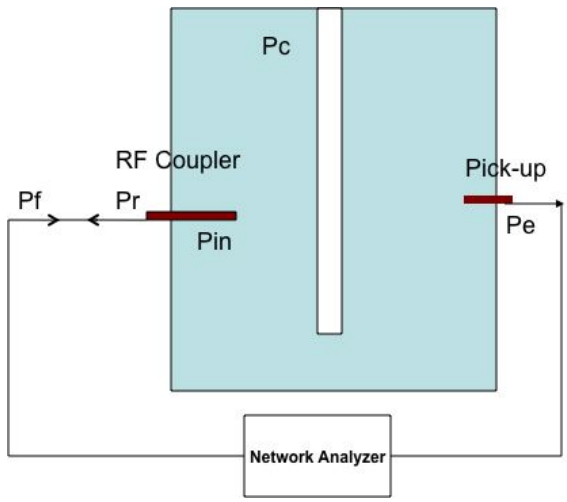

Figure 9: Q_{ext} measurements: Pf stands for forward power, Pr is the reflected power, Pin is the power inside the cavity, Pc the dissipated power on the cavity wall and Pe is the output power from pick-up.

Table 3 shows some measurements: yellow line is a Q_0 measurement by a S11 without pick-up. The value of the Q_0 should stay the same in the this condition of measurement. Then the precision of this method can be roughly estimated by evaluating the maximum variation of Q_0 which is of 3.6%.

Table 3: Measurement results, yellow line is a Q_0 measurement by a S11 without pick-up.

Pick-up insertion (mm)	β_c	β_{pu}	Q_0	Q_{pu}
W/O	1.019	-	11380	-
22	1.73	0.0557	10870	$1.95\cdot10^5$
	0.96	0.0565	11085	$1.96\cdot10^5$
-1	1.84	0.0003	11204	$3.66\cdot10^7$
	1.016	0.0003	11376	$3.7\cdot10^7$

CONCLUSIONS

The coupler line for the first cavity prototype of HIE-ISOLDE has been fully studied and characterized. The analytical analysis of the line has been developed. We have paid particular attention to the ohmic losses. The final results will be taken into considerations for the design of the cryomodule as additional cryogenic losses.

The final layout of the line could be slightly changed without affecting significantly the results here presented.

Finally we have also presented the method we use to measure the very high values of Q_{ext} of the coupler and pick-up by means of a simple S21 measurement. This method is very helpful to have a measurement of high Q_{ext} (up to $\approx 10^{10}$) of the coupler and pick-up when the cavity is normal condcting ($Q_0 \approx 10^4$). Some first measurements have been presented showing a precision of $\approx$4% of the method.

ACKNOWLEDGEMENTS

The authors wish to thank the Cockroft Institute for supporting this project. We are also thankful to Gilles Villiger for the mechanical design of the coupler.

REFERENCES

[1] M. Pasini "HIE-Isolde: The Superconducting RIB Linac at CERN", these proceedings.

[2] G. Lanza et al., "The HIE-ISOLDE Superconducting Cavities: Surface Treatment and Niobium Thin Film Coating", these proceedings.

[3] A. D'Elia et al., "HIE-ISOLDE High Beta Cavity Study and Measurement", these proceedings.

[4] T. Ries et al., "A Mechanical Tuner for the ISAC-II Quarter Wave Superconducting Cavities", TRIPP0322, May 2003.

[5] G. Bisoffi, private communication.

[6] www.cst.com/

[7] V. Zvyagintsev, "RF calculations of the coupler line for ISAC-II Superconductive Quarter Wave Resonators", TRI-DN-04-13, June 2004.

[8] A. D'Elia, "Design and realization of the power coupler for HIE-ISOLDE", in preparation.